

See discussions, stats, and author profiles for this publication at: <https://www.researchgate.net/publication/5413949>

# Neutral Gold(I) Metallosupramolecular Compounds: Synthesis and Characterization, Photophysical Properties, and Density Functional Theory Studies

ARTICLE *in* INORGANIC CHEMISTRY · JUNE 2008

Impact Factor: 4.76 · DOI: 10.1021/ic800266m · Source: PubMed

---

CITATIONS

21

READS

44

## 4 AUTHORS:



Laura Rodríguez

University of Barcelona

58 PUBLICATIONS 615 CITATIONS

[SEE PROFILE](#)



Carlos Lodeiro

University NOVA of Lisbon

241 PUBLICATIONS 3,042 CITATIONS

[SEE PROFILE](#)



João Carlos Lima

New University of Lisbon

143 PUBLICATIONS 2,221 CITATIONS

[SEE PROFILE](#)



Ramon Crehuet

Spanish National Research Council

46 PUBLICATIONS 696 CITATIONS

[SEE PROFILE](#)

# Neutral Gold(I) Metallosupramolecular Compounds: Synthesis and Characterization, Photophysical Properties, and Density Functional Theory Studies

Laura Rodríguez,<sup>\*,†,‡</sup> Carlos Lodeiro,<sup>†</sup> João Carlos Lima,<sup>†</sup> and Ramon Crehuet<sup>§</sup>

REQUIMTE, Departamento de Química, Centro de Química Fina e Biotecnologia, Universidade Nova de Lisboa, Quinta da Torre, 2829-516 Monte de Caparica, Portugal, Departament de Química Inorgànica, Universitat de Barcelona, Martí i Franquès 1-11, 08028 Barcelona, Spain, and Institut d'Investigacions Químiques i Ambientals de Barcelona, IIQAB-CSIC, c/ Jordi Girona 18-26, Barcelona 08034, Spain

Received February 11, 2008

The reaction of the tris-indole InTREN ligand (L) with different gold phosphine fragments allows the construction of new gold(I) complexes with different geometries depending on the chosen phosphine. A metallocryptand structure is obtained when the gold atom is linked to a triphenylphosphine ligand, and neutral gold(I) metallosupramolecules are constructed when a triphosphine is used. Characterization of the compounds was accomplished by  $^{31}\text{P}\{\text{H}\}$  and  $^1\text{H}$  NMR, IR, absorption, and fluorescence spectroscopies, electrospray ionization mass spectrometry (ESI-MS(+)), and elemental analysis, and their geometry was optimized using density functional theory (B3LYP). Time-dependent density functional theory (TD-DFT) calculations have been used to assign the lowest energy absorption bands to LMCT N(p, tertiary amine) → Au transitions. Photophysical characterization of the complexes shows strong luminescence in the solid state. The formation of heterobimetallic species has been detected in solution in the presence of equimolar quantities of metal cations, and their structures have been identified by a combination of spectroscopic methods and mass spectrometry.

## Introduction

The construction of metallosupramolecular structures using transition metal centers and coordination bonds, for the direct formation of complex structures, has undergone significant development for more than one decade. It has proved to be an efficient method to obtain molecular compounds with a wide range of shapes and sizes, which can be controlled by the rational choice of the appropriate metals and ligands.<sup>1–11</sup>

Although there are numerous examples of metal-mediated self-assembly bidimensional complexes, especially with square<sup>9,12–22</sup> and rectangular<sup>10,23–28</sup> shape, the design of three-dimensional structures is more scarce, in particular involving synthetic structures from typically inorganic build-

\* To whom correspondence should be addressed. E-mail: l.raurell@dq.fct.unl.pt. Phone: +351 212948300 (Ext. 10981). Fax: +351 212948550.

<sup>†</sup> Universidade Nova de Lisboa.

<sup>‡</sup> Universitat de Barcelona.

<sup>§</sup> Institut d'Investigacions Químiques i Ambientals de Barcelona.

- (1) Chen, C.-L.; Zhang, J. Y.; Su, C.-Y. *Eur. J. Inorg. Chem.* **2007**, 2997–3010.
- (2) Jones, C. J. *Chem. Soc. Rev.* **1998**, 27, 289–299.
- (3) Fujita, M. *Chem. Soc. Rev.* **1998**, 27, 417–425.
- (4) Swiegers, G. F.; Malefetse, T. J. *Chem. Rev.* **2000**, 100, 3483–3537.
- (5) Leininger, S.; Olenyuk, B.; Stang, P. J. *Chem. Rev.* **2000**, 100, 853–907.
- (6) Holliday, B. J.; Mirkin, C. A. *Angew. Chem., Int. Ed.* **2001**, 40, 2022–2043.
- (7) Stang, P. J. *Chem.—Eur. J.* **1998**, 4, 19–27.

- (8) Schalley, C. A.; Lutzen, A.; Albrecht, M. *Chem.—Eur. J.* **2004**, 10, 1072–1080.
- (9) Wurthner, F.; You, C. C.; Saha-Moller, C. R. *Chem. Soc. Rev.* **2004**, 33, 133–146.
- (10) Thanasekaran, P.; Liao, R. T.; Liu, Y. H.; Rajendran, T.; Rajagopal, S.; Lu, K. L. *Coord. Chem. Rev.* **2005**, 249, 1085–1110.
- (11) Ghosh, S.; Batten, S. R.; Turner, D. R.; Mukherjee, P. S. *Organometallics* **2007**, 26, 3252–3255.
- (12) Bera, J. K.; Bacsá, J.; Smucker, B. W.; Dunbar, K. R. *Eur. J. Inorg. Chem.* **2004**, 368–375.
- (13) Ferrer, M.; Rodriguez, L.; Rossell, O.; Solans, X. J. *Organomet. Chem.* **2005**, 690, 1612–1619.
- (14) Kraft, S.; Hanuschek, E.; Beckhaus, R.; Haase, D.; Saak, W. *Chem.—Eur. J.* **2005**, 11, 969–978.
- (15) Song, L. C.; Jin, G. X.; Wang, H. T.; Zhang, W. X.; Hu, Q. M. *Organometallics* **2005**, 24, 6464–6471.
- (16) Karadas, F.; Scheiter, E. J.; Prosvirin, A. V.; Bacsá, J.; Dunbar, K. R. *Chem. Commun.* **2005**, 1414–1416.
- (17) Sautter, A.; Kaletas, B. K.; Schmid, D. G.; Dobrawa, R.; Zimine, M.; Jung, G.; van Stokkum, I. H. M.; De Cola, L.; Williams, R. M.; Wurthner, F. *J. Am. Chem. Soc.* **2005**, 127, 6719–6729.

ing blocks.<sup>29–37</sup> It is interesting to note that the assembly of three-dimensional compounds using metal coordination presents additional challenging and interesting applications in the area of chemical nanosciences, being used as supramolecular containers, reaction vessels, and ion channel models for biological cells.<sup>38</sup>

Metallocryptands are an emerging class of inorganic three-dimensional cage complexes that are well-suited to encapsulate a variety of metal ions.<sup>39</sup> Unlike their more common organic analogues, these complexes have the possibility of binding metal ions either by the formation of metalophilic interactions or by Lewis base interactions with the electron donor groups of the ligands. Although the synthesis of cationic gold(I) metallocryptates has been carried out by Catalano et al.,<sup>39–44</sup> there are no examples in the literature, to our knowledge, of neutral gold(I) metallocryptands constructed directly in a one-step reaction between two tripodal precursors.

- (18) Jude, H.; Disteldorf, H.; Fischer, S.; Wedge, T.; Hawkridge, A. M.; Arif, A. M.; Hawthorne, M. F.; Muddiman, D. C.; Stang, P. J. *J. Am. Chem. Soc.* **2005**, *127*, 12131–12139.
- (19) Cotton, F. A.; Murillo, C. A.; Yu, R. M. *Dalton Trans.* **2006**, 3900–3905.
- (20) Ferrer, M.; Rodríguez, L.; Rossell, O. *J. Organomet. Chem.* **2003**, *681*, 158–166.
- (21) Ferrer, M.; Gutiérrez, A.; Mounir, M.; Rossell, O.; Ruiz, E.; Rang, A.; Engeser, M. *Inorg. Chem.* **2007**, *46*, 3395–3406.
- (22) Ferrer, M.; Mounir, M.; Rossell, O.; Ruiz, E.; Maestro, M. A. *Inorg. Chem.* **2003**, *42*, 5890–5899.
- (23) Mukherjee, P. S.; Min, K. S.; Arif, A. M.; Stang, P. J. *Inorg. Chem.* **2004**, *43*, 6345–6350.
- (24) Dinolfo, P. H.; Hupp, J. T. *J. Am. Chem. Soc.* **2004**, *126*, 16814–16819.
- (25) Han, W. S.; Lee, S. W. *Dalton Trans.* **2004**, 1656–1663.
- (26) Lin, R.; Yip, J. H. K.; Zhang, K.; Koh, L. L.; Wong, K. Y.; Ho, K. P. *J. Am. Chem. Soc.* **2004**, *126*, 15852–15869.
- (27) Addicott, C.; Oesterling, I.; Yamamoto, T.; Mullen, K.; Stang, P. J. *J. Org. Chem.* **2005**, *70*, 797–801.
- (28) Cornpany, A.; Gomez, L.; Valbuena, J. M. L.; Mas-Balleste, R.; Benet-Buchholz, J.; Llobet, A.; Costas, M. *Inorg. Chem.* **2006**, *45*, 2501–2508.
- (29) Reger, D. L.; Semeniuc, R. F.; Smith, M. D. *Inorg. Chem.* **2003**, *42*, 8137–8139.
- (30) Ghosh, S.; Mukherjee, P. S. *J. Org. Chem.* **2006**, *71*, 8412–8416.
- (31) Fujita, M.; Oguro, D.; Miyazawa, M.; Oka, H.; Yamaguchi, K.; Ogura, K. *Nature* **1995**, *378*, 469–471.
- (32) Kobayashi, K.; Yamada, Y.; Yamanaka, M.; Sei, Y.; Yamaguchi, K. *J. Am. Chem. Soc.* **2004**, *126*, 13896–13897.
- (33) Paul, R. L.; Argent, S. P.; Jeffery, J. C.; Harding, L. P.; Lynam, J. M.; Ward, M. D. *Dalton Trans.* **2004**, 3453–3458.
- (34) Pinalli, R.; Cristini, V.; Sottili, V.; Geremia, S.; Campagnolo, M.; Caneschi, A.; Dalcanale, E. *J. Am. Chem. Soc.* **2004**, *126*, 6516–6517.
- (35) Yoshizawa, M.; Nakagawa, N.; Kumazawa, K.; Nagao, M.; Kawano, M.; Ozeki, T.; Fujita, M. *Angew. Chem., Int. Ed.* **2005**, *44*, 1810–1813.
- (36) Liu, Z.-M.; Liu, Y.; Zheng, S.-R.; Yu, Z.-Q.; Pan, M.; Su, C.-Y. *Inorg. Chem.* **2007**, *46*, 5814–5816.
- (37) Dertz, E. A.; Xu, J. D.; Raymond, K. N. *Inorg. Chem.* **2006**, *45*, 5465–5478.
- (38) Cronin, L. *Angew. Chem., Int. Ed.* **2006**, *45*, 3576–3578.
- (39) Catalano, V. J.; Bennett, B. L.; Malwitz, M. A.; Yson, R. L.; Kar, H. M.; Muratidis, S.; Horner, S. J. *Comments Inorg. Chem.* **2003**, *24*, 39–68.
- (40) Catalano, V. J.; Malwitz, M. A.; Noll, B. C. *Chem. Commun.* **2001**, 581–582.
- (41) Catalano, V. J.; Bennett, B. L.; Kar, H. M.; Noll, B. C. *J. Am. Chem. Soc.* **1999**, *121*, 10235–10236.
- (42) Catalano, V. J.; Malwitz, M. A. *J. Am. Chem. Soc.* **2004**, *126*, 6560–6561.
- (43) Catalano, V. J.; Malwitz, M. A.; Horner, S. J.; Vasquez, J. *Inorg. Chem.* **2003**, *42*, 2141–2148.
- (44) Catalano, V. J.; Bennett, B. L.; Yson, R. L.; Noll, B. C. *J. Am. Chem. Soc.* **2000**, *122*, 10056–10062.

The affinity of gold for the nitrogen atoms, in comparison with that for phosphorus or sulfur, is low, but a number of neutral or ionic gold complexes with gold(I)–nitrogen bonds in the presence of P-donor ligands have been reported.<sup>45–48</sup> Furthermore, because of the ability of the indole ligands to react with gold metal atoms,<sup>49</sup> we have explored the reaction of the new InTREN ligand<sup>50</sup> with different gold phosphine derivatives leading to the formation of one complex with dendrimeric structure and two new neutral gold(I) metallocryptands with closed-shell geometry.

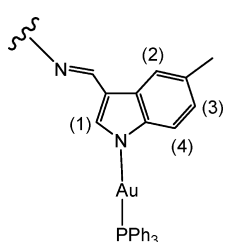
## Experimental Section

**General.** All manipulations were performed under prepurified N<sub>2</sub> using standard Schlenk techniques. All solvents were distilled from the appropriate drying agents. The compounds InTREN,<sup>50</sup> AuClPPh<sub>3</sub>,<sup>51</sup> Tl(acac),<sup>52</sup> Au(acac)PPh<sub>3</sub>,<sup>52</sup> and InTREN<sup>50</sup> were synthesized as described previously. The compounds (AuCl)<sub>3</sub>(triphos) and (AuCl)<sub>3</sub>(tripod) were prepared and isolated as solids from AuCl(tht)<sup>53</sup> solutions by adding the appropriate amount of the corresponding triphosphine. Zn(OTf)<sub>2</sub> (Aldrich, 98%), Cu(OTf)<sub>2</sub> (Aldrich, 98%), and Ni(BF<sub>4</sub>)<sub>2</sub> (Strem Chemicals, 99%) were used as received.

**Measurements.** IR spectra were recorded on an FT-IR 520 Nicolet spectrophotometer. <sup>31</sup>P{<sup>1</sup>H}-NMR ( $\delta$  (85% H<sub>3</sub>PO<sub>4</sub>) = 0.0 ppm) and <sup>1</sup>H NMR ( $\delta$  (TMS) = 0.0 ppm) spectra were obtained on Bruker DXR 250 and Varian Mercury 400 spectrometers. Elemental analyses of C, H, and N were carried out at the Serveis Científico-Tècnics of the Universitat de Barcelona. Electrospray ionization mass spectrometry (ESI-MS) spectra were recorded on a LC/MSD-TOF spectrometer at the Universitat de Barcelona and matrix-assisted laser desorption ionization time-of-flight (MALDI-TOF) spectra on a Voyager DE-PRO Biospectrometry Workstation equipped with a nitrogen laser radiating at 337 nm (Applied Biosystems, Foster City, CA) in the laboratory of mass spectrometry of the REQUIMTE-UNL. Absorption spectra were recorded on a Shimadzu UV-2501PC spectrophotometer and fluorescence emission spectra on a Horiba-Jobin-Yvon SPEX Fluorolog 3.22 spectrofluorimeter at 25 °C. Emission spectra in the solid state were recorded using a Fiberoptic Adaptor model F-3000.

**Computational Details.** Because of the large size of the system, the calculations have been carried out on a simplified model of the molecules. The indole group of the InTREN has been converted into a pyrrole group, and phenyl groups have been substituted with methyl groups, for compounds **2** and **3**. For compound **1**, it was necessary to retain the phenyl rings, as these rings strongly determine its conformation (vide infra). The use of methyl groups instead of the simpler hydrogen atoms gives results for geometric and electronic properties closer to experimental values.<sup>54</sup> We have used the LanL2DZ basis set<sup>55,56</sup> for the Au and P atoms and the

- (45) Nomiya, K.; Noguchi, R.; Ohsawa, K.; Tsuda, K.; Oda, M. *J. Inorg. Biochem.* **2000**, *78*, 363–370.
- (46) Nomiya, K.; Noguchi, R.; Oda, M. *Inorg. Chim. Acta* **2000**, *298*, 24–32.
- (47) Nomiya, K.; Noguchi, R.; Ohsawa, K.; Tsuda, K. *J. Chem. Soc., Dalton Trans.* **1998**, 4101–4108.
- (48) Munakata, M.; Yan, S. G.; Maekawa, M.; Akiyama, M.; Kitagawa, S. *J. Chem. Soc., Dalton Trans.* **1997**, 4257–4262.
- (49) Usón, R.; Oro, L. A.; Cabeza, J. A.; Valderrama, M. *J. Organomet. Chem.* **1982**, *231*, C81–C83.
- (50) Oliveira, E.; Pedras, B.; Santos, H.; Rodríguez, L.; Crehuet, R.; Avilés, T.; Capelo, J. L.; Lodeiro, C. Manuscript in preparation.
- (51) Kowala, C.; Swan, J. M. *Aust. J. Chem.* **1966**, *19*, 547.
- (52) Vicente, J.; Chicote, M. T. *Inorg. Synth.* **1998**, *32*, 172.
- (53) Usón, R.; Laguna, A. *Organomet. Synth.* **1986**, *3*, 322.

**Scheme 1**

D95V basis set<sup>57</sup> for the remaining atoms. Additional f and d polarization functions were added to Au ( $\alpha_f = 0.2$ ) and P ( $\alpha_f = 0.34$ ), respectively.<sup>58</sup>

Ground-state structures were optimized without symmetry constraints in the gas phase. The time-dependent density functional theory (TD-DFT) calculations included the solvent effect via the polarizable continuum model<sup>59</sup> using the gas phase geometries. Twenty-five singlet excited states were calculated. To check the influence of the basis set, single point TD-DFT calculations with solvent for compound **3** were repeated using the LanL2DZdp basis set, which includes polarization and diffuse functions for all the atoms.<sup>60</sup> All calculations have been performed using the B3LYP functional and the program Gaussian03.<sup>61</sup> Gabedit was used to generate the graphical three-dimensional representations of the orbitals.<sup>62</sup>

**Synthesis of (InTREN)(AuPPh<sub>3</sub>)<sub>3</sub> (1).** **Method A.** A methanol solution (2 mL) of InTREN (10 mg, 0.02 mmol) and potassium hydroxide (4 mg, 0.07 mmol) was stirred at room temperature for 30 min. Then, a dichloromethane solution (2 mL) of AuClPPh<sub>3</sub> (26 mg, 0.05 mmol) was added. After 2 h of stirring, the solvent was concentrated in vacuum to a final volume of 2 mL, and hexane (6 mL) was added. A pale orange solid was obtained, filtered, washed with diethyl ether and hexane, and vacuum-dried. During all the manipulations, the solution was protected from the light in order to avoid decomposition. Yield: 92%. <sup>31</sup>P NMR (CH<sub>2</sub>Cl<sub>2</sub>, inset acetone-*d*<sub>6</sub> with 1% POMe<sub>3</sub>):  $\delta$  31.4. <sup>1</sup>H NMR (CD<sub>2</sub>Cl<sub>2</sub>):  $\delta$  8.35 (s, 3H, CH<sub>2</sub>-N-CH), 7.89 (s, 3H, H<sub>1,indole</sub>, Scheme 1), 7.52–7.41 (m, 48H, Ph + H<sub>4,indole</sub>), 6.78 (s, 3H, H<sub>2,indole</sub>), 6.75 (s, br, 3H, H<sub>3,indole</sub>), 3.62 (s, br, 6H, CH<sub>2</sub>-N-CH), 2.89 (s, br, 6H, CH<sub>2</sub>-CH<sub>2</sub>-N-CH), 2.31 (s, 9H, CH<sub>3</sub>). IR (KBr, cm<sup>-1</sup>): 3239 w, br (N-H); 3050 w, 2917 w, 2811 w (C-H); 1639 s, 1624 vs, 1617 s, (indole); 1476 m, 1436 s, 1101 s (PPh<sub>3</sub>). ESI-MS (CH<sub>2</sub>Cl<sub>2</sub>, *m/z*): 1945.2 (M + H<sup>+</sup>, calcd: 1945.4), 1487.8 (M - AuPPh<sub>3</sub> + 2H<sup>+</sup>, calcd: 1487.5), 1410.6 (M - AuPPh<sub>3</sub> - Ph + 2H<sup>+</sup>, calcd: 1410.5), 1029.7 (M - 2AuPPh<sub>3</sub> + 3H<sup>+</sup>, calcd: 1029.5), 973.4 (M + 2H<sup>+</sup>, calcd: 972.8), 722.4 (M - 2AuPPh<sub>3</sub> - PPh<sub>3</sub> - 3CH<sub>3</sub> + 3H<sup>+</sup>, calcd: 722.6), 649.3 (M + 3H<sup>+</sup>, calcd: 648.8), 570.7 (InTREN + H<sup>+</sup>, calcd: 570.7). Anal. Calcd: C, 55.59; H, 4.20; N, 5.04. Found: C, 55.62; H, 4.25; N, 5.09.

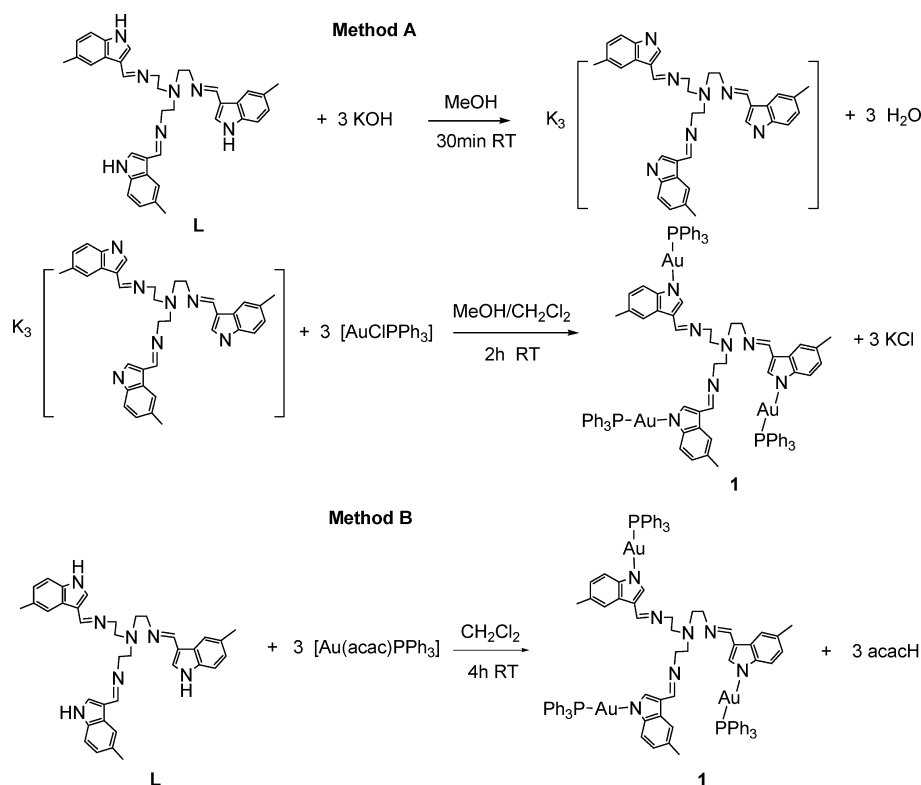
**Method B.** A dichloromethane solution (4 mL) of [Au(acac)-PPh<sub>3</sub>] (55 mg, 0.10 mmol) was added dropwise to a dichloromethane solution (6 mL) of InTREN (19 mg, 0.03 mmol). After 4 h of stirring at room temperature, the solution was filtered through anhydrous magnesium sulfate and concentrated to a final volume of 2 mL, and then hexane (6 mL) was added. A pale orange solid was obtained, filtered, washed with diethyl ether and hexane, and vacuum-dried. During all the manipulations, the solution was protected from the light in order to avoid decomposition. Yield: 90%. <sup>31</sup>P NMR (CH<sub>2</sub>Cl<sub>2</sub>, inset acetone-*d*<sub>6</sub> with 1% POMe<sub>3</sub>):  $\delta$  31.4. <sup>1</sup>H NMR (CD<sub>2</sub>Cl<sub>2</sub>):  $\delta$  8.35 (s, 3H, CH<sub>2</sub>-N-CH), 7.89 (s, 3H, H<sub>1,indole</sub>, Scheme 1), 7.52–7.41 (m, 48H, Ph + H<sub>4,indole</sub>), 6.78 (s, 3H, H<sub>2,indole</sub>), 6.75 (s, br, 3H, H<sub>3,indole</sub>), 3.62 (s, br, 6H, CH<sub>2</sub>-N-CH), 2.89 (s, br, 6H, CH<sub>2</sub>-CH<sub>2</sub>-N-CH), 2.31 (s, 9H, CH<sub>3</sub>). IR (KBr, cm<sup>-1</sup>): 3239 w, br (N-H); 3050 w, 2917 w, 2811 w (C-H); 1639 s, 1624 vs, 1617 s, (indole); 1476 m, 1436 s, 1101 s (PPh<sub>3</sub>). ESI-MS (CH<sub>2</sub>Cl<sub>2</sub>, *m/z*): 1945.2 (M + H<sup>+</sup>, calcd: 1945.4), 1487.8 (M - AuPPh<sub>3</sub> + 2H<sup>+</sup>, calcd: 1487.5), 1410.6 (M - AuPPh<sub>3</sub> - Ph + 2H<sup>+</sup>, calcd: 1410.5), 1029.7 (M - 2AuPPh<sub>3</sub> + 3H<sup>+</sup>, calcd: 1029.5), 973.4 (M + 2H<sup>+</sup>, calcd: 972.8), 722.4 (M - 2AuPPh<sub>3</sub> - PPh<sub>3</sub> - 3CH<sub>3</sub> + 3H<sup>+</sup>, calcd: 722.6), 649.3 (M + 3H<sup>+</sup>, calcd: 648.8), 570.7 (InTREN + H<sup>+</sup>, calcd: 570.7). Anal. Calcd: C, 55.59; H, 4.20; N, 5.04. Found: C, 55.62; H, 4.25; N, 5.09.

**Synthesis of (Triphos)Au<sub>3</sub>(InTREN) (2).** **Method A.** A methanol solution (4 mL) of InTREN (9 mg, 0.02 mmol) and potassium hydroxide (4 mg, 0.07 mmol) was stirred at room temperature for 30 min. Then, a dichloromethane solution (3 mL) of (triphos)-(AuCl)<sub>3</sub> (20 mg, 0.02 mmol) was added. A pale orange solid was obtained after 1 h of stirring. The solid was filtered, washed with hexane and diethyl ether, and vacuum-dried. During all the manipulations, the solution was protected from the light in order to avoid decomposition. Yield: 93%. <sup>31</sup>P NMR (CH<sub>2</sub>Cl<sub>2</sub>, inset acetone-*d*<sub>6</sub> with 1% POMe<sub>3</sub>):  $\delta$  17.2. <sup>1</sup>H NMR (DMSO-*d*<sub>6</sub>):  $\delta$  8.31 (s, 3H, CH<sub>2</sub>-N-CH), 7.99 (s, 3H, H<sub>1,indole</sub>), 7.78–7.65 (m, 30H, Ph), 7.62 (s, br, 3H, H<sub>4,indole</sub>), 7.22 (s, 3H, H<sub>2,indole</sub>), 6.62 (s, br, 3H, H<sub>3,indole</sub>), 4.13 (s, br, 6H, CH<sub>2</sub>-N-CH), 3.50 (s, br, 6H, CH<sub>2</sub>-CH<sub>2</sub>-N-CH), 3.12 (s, br, 6H, CH<sub>2</sub>-P), 2.32 (s, 9H, CH<sub>3</sub>), 1.60 (s, 3H, CH<sub>3</sub>-C-). IR (KBr, cm<sup>-1</sup>): 3253 w, br (N-H); 3047 w, 2921 w, 2844 w, 2811 w (C-H); 1655 s, 1642 s, 1639 s, 1627 s, 1612 s, 1383 s (indole); 1476 m, 1436 s, 1101 s (PPh<sub>2</sub>). ESI-MS (CH<sub>2</sub>Cl<sub>2</sub>, *m/z*): 1782.6 (M + H<sup>+</sup>, calcd: 1782.4), 892.2 (M + 2H<sup>+</sup>, calcd: 891.7), 595.2 (M + 3H<sup>+</sup>, calcd: 594.8). Anal. Calcd: C, 51.89; H, 4.24; N, 5.50. Found: C, 51.93; H, 4.29; N, 5.54.

**Method B.** A dichloromethane solution (6 mL) of [{Au(acac)}<sub>3</sub>-(triphos)] (25 mg, 0.17 mmol; following the same procedure as for the PPh<sub>3</sub> gold derivative<sup>52</sup>) was added dropwise to a dichloromethane solution (8 mL) of InTREN (9.4 mg, 0.17 mmol). After 4 h of stirring at room temperature, the solution was filtered through anhydrous magnesium sulfate and concentrated to a final volume of 2 mL, and then hexane (8 mL) was added. A pale orange solid was obtained, filtered, washed with diethyl ether and hexane, and

- (54) Bardaji, M.; Calhorda, M. J.; Costa, P. J.; Jones, P. G.; Laguna, A.; Perez, M. R.; Villacampa, M. D. *Inorg. Chem.* **2006**, *45*, 1059–1068.
- (55) Hay, P. J.; Wadt, W. R. *J. Chem. Phys.* **1985**, *82*, 270–283.
- (56) Wadt, W. R.; Hay, P. J. *J. Chem. Phys.* **1985**, *82*, 284–298.
- (57) Dunning, T. H., Jr.; Hay, P. J. In *Modern Theoretical Chemistry*; Schaefer, H. F., III, Ed.; Plenum: New York, 1976.
- (58) Pyykko, P.; Runeberg, N.; Mendizabal, F. *Chem.-Eur. J.* **1997**, *3*, 1451–1457.
- (59) Tomasi, J.; Mennucci, B.; Cammi, R. *Chem. Rev.* **2005**, *105*, 2999–3093.
- (60) Check, C. E.; Faust, T. O.; Bailey, J. M.; Wright, B. J.; Gilbert, T. M.; Sunderlin, L. S. *J. Phys. Chem. A* **2001**, *105*, 8111–8116.
- (61) Frisch, M. J. T. G. W.; Schlegel, H. B.; Scuseria, G. E.; Robb, M. A.; Cheeseman, J. R.; Montgomery, J. A., Jr.; Vreven, T.; Kudin, K. N.; Burant, J. C.; Millam, J. M.; Iyengar, S. S.; Tomasi, J.; Barone, V.; Mennucci, B.; Cossi, M.; Scalmani, G.; Rega, N.; Petersson, G. A.; Nakatsuji, H.; Hada, M.; Ehara, M.; Toyota, K.; Fukuda, R.; Hasegawa, J.; Ishida, M.; Nakajima, T.; Honda, Y.; Kitao, O.; Nakai, H.; Klene, M.; Li, X.; Knox, J. E.; Hratchian, H. P.; Cross, J. B.; Bakken, V.; Adamo, C.; Jaramillo, J.; Gomperts, R.; Stratmann, R. E.; Yazyev, O.; Austin, A. J.; Cammi, R.; Pomelli, C.; Ochterski, J. W.; Ayala, P. Y.; Morokuma, K.; Voth, G. A.; Salvador, P.; Dannenberg, J. J.; Zakrzewski, V. G.; Dapprich, S.; Daniels, A. D.; Strain, M. C.; Farkas, O.; Malick, D. K.; Rabuck, A. D.; Raghavachari, K.; Foresman, J. B.; Ortiz, J. V.; Cui, Q.; Baboul, A. G.; Clifford, S.; Cioslowski, J.; Stefanov, B. B.; Liu, G.; Liashenko, A.; Piskorz, P.; Komaromi, I.; Martin, R. L.; Fox, D. J.; Keith, T.; Al-Laham, M. A.; Peng, C. Y.; Nanayakkara, A.; Challacombe, M.; Gill, P. M. W.; Johnson, B.; Chen, W.; Wong, M. W.; Gonzalez, C.; Pople, J. A. *Gaussian 03*, Revision C.02; Gaussian, Inc.: Wallingford, CT, 2004.
- (62) <http://gabedit.sourceforge.net/home.htm>.

Scheme 2



vacuum-dried. During all the manipulations, the solution was protected from the light in order to avoid decomposition. Yield: 90%.  $^{31}\text{P}$  NMR ( $\text{CH}_2\text{Cl}_2$ , inset acetone- $d_6$  with 1%  $\text{POMe}_3$ ):  $\delta$  17.2.  $^1\text{H}$  NMR ( $\text{DMSO}-d_6$ ):  $\delta$  8.31 (s, 3H,  $\text{CH}_2-\text{N}-\text{CH}$ ), 7.99 (s, 3H,  $\text{H}_{1,\text{indole}}$ ), 7.78–7.65 (m, 30H, Ph), 7.62 (s, br, 3H,  $\text{H}_{4,\text{indole}}$ ), 7.22 (s, 3H,  $\text{H}_{2,\text{indole}}$ ), 6.62 (s, br, 3H,  $\text{H}_{3,\text{indole}}$ ), 4.13 (s, br, 6H,  $\text{CH}_2-\text{N}-\text{CH}$ ), 3.50 (s, br, 6H,  $\text{CH}_2-\text{CH}_2-\text{N}-\text{CH}$ ), 3.12 (s, br, 6H,  $\text{CH}_2-\text{P}$ ), 2.32 (s, 9H,  $\text{CH}_3$ ), 1.60 (s, 3H,  $\text{CH}_3-\text{C}-$ ). IR (KBr,  $\text{cm}^{-1}$ ): 3253 w, br (N–H); 3047 w, 2921 w, 2844 w, 2811 w (C–H); 1655 s, 1642 s, 1639 s, 1627 s, 1612 s, 1383 s (indole); 1476 m, 1436 s, 1101 s ( $\text{PPh}_2$ ). ESI-MS ( $\text{CH}_2\text{Cl}_2$ ,  $m/z$ ): 1782.6 (M +  $\text{H}^+$ , calcd: 1782.4), 892.2 (M + 2 $\text{H}^+$ , calcd: 891.7), 595.2 (M + 3 $\text{H}^+$ , calcd: 594.8). Anal. Calcd: C, 51.89; H, 4.24; N, 5.50. Found: C, 51.93; H, 4.29; N, 5.54.

**Synthesis of (Tripod) $\text{Au}_3(\text{InTREN})$  (3).** A similar procedure was followed for the synthesis of **2**, using the previously synthesized  $\{\{\text{Au}(\text{acac})\}_{\text{(tripod)}}\}$  derivative by the same method as for  $\text{PPh}_3$ .<sup>52</sup> Yield: 90%.  $^{31}\text{P}$  NMR ( $\text{CH}_2\text{Cl}_2$ , inset acetone- $d_6$  with 1%  $\text{POMe}_3$ ):  $\delta$  37.3.  $^1\text{H}$  NMR ( $\text{CD}_2\text{Cl}_2-d_6$ ):  $\delta$  8.34 (s, 3H,  $\text{CH}_2-\text{N}-\text{CH}$ ), 8.17 (s, 3H,  $\text{H}_{1,\text{indole}}$ ), 7.83 (d,  $J(\text{H}-\text{H}) = 8.2$  Hz, 3H,  $\text{H}_{4,\text{indole}}$ ), 7.68 (s, 3H,  $\text{H}_{2,\text{indole}}$ ), 7.48–6.82 (m, 30H, Ph), 7.06 (s, 3H,  $\text{H}_{3,\text{indole}}$ ), 5.48 (s, 1H,  $\text{HC}-(\text{PPh}_2)_3$ ), 3.67 (s, br, 6H,  $\text{CH}_2-\text{N}-\text{CH}$ ), 2.93 (s, br, 6H,  $\text{CH}_2-\text{CH}_2-\text{N}-\text{CH}$ ), 2.44 (s, 9H,  $\text{CH}_3$ ). IR (KBr,  $\text{cm}^{-1}$ ): 3236 w, br (N–H); 3050 w, 2920 w, 2854 w, 2821 w (C–H); 1652 s, 1642 s, 1635 vs, 1617 s, 1384 vs (indole); 1476 m, 1437 s, 1094 m ( $\text{PPh}_2$ ). ESI-MS ( $\text{CH}_2\text{Cl}_2$ ,  $m/z$ ): 1727.0 (M +  $\text{H}^+$ , calcd: 1727.1), 863.8 (M + 2 $\text{H}^+$ , calcd: 864.0), 576.0 (M + 3 $\text{H}^+$ , calcd: 576.3). Anal. Calcd: C, 50.79; H, 3.91; N, 5.68. Found: C, 50.83; H, 3.96; N, 5.73.

## Results and Discussion

**Syntheses and Characterizations.** The well-known ability of an indole group to act as an N-donor ligand in transition

metal complexes<sup>49,63</sup> has been used to explore the reactivity of the InTREN ligand (**L**) with different gold(I) phosphine compounds. Treatment of **L** with 3 equiv of  $\text{AuPPh}_3^+$  leads to the obtention of compound **1**, with dendrimer-like structure. The synthesis of **1** has been carried out by two different methods (Scheme 2). Method A had been employed many years ago by Usón et al.<sup>49</sup> and is based on the treatment of **L** with KOH in MeOH for 30 min. The obtained potassium indole salt gives **1** after addition of a stoichiometric amount of  $\text{AuClPPh}_3$ . Addition of some  $\text{CH}_2\text{Cl}_2$  is required in order to improve the solubility of the products in the reaction medium.

Following the “acac method”,<sup>64</sup> we have used the acetyl-acetonato gold derivative  $[\text{Au}(\text{acac})\text{PPh}_3]$  in the reaction with **L** (Method B, Scheme 2). In this synthetic procedure, the deprotonation of the indole nitrogen atom and the formation of the indole–gold bond are accomplished in only one step. Although higher reaction times are needed in method B, less manipulation is required, and the compound is obtained in similar yield. Characterization of the solid by NMR and IR spectroscopies and mass spectrometry confirmed the formation of the product. The  $^1\text{H}$  NMR spectrum shows that the protons of the indolyl groups are moved upfield ( $\sim 0.2$  ppm) upon the coordination of the gold fragment.  $^{31}\text{P}$  NMR led us to verify the formation of a symmetrical compound and showed the coordination of all the  $\text{AuPPh}_3^+$  fragments, since it displays a single resonance at 31.3 ppm, which is shifted upfield about 7 ppm relative to the corresponding  $[\text{Au}(\text{acac})\text{PPh}_3]$  precursor or 2 ppm from the  $[\text{AuCl}(\text{PPh}_3)]$ .

(63) Pauson, P. L.; Qazi, A. R. *J. Organomet. Chem.* **1967**, 7 (2), 321.

(64) Vicente, J.; Chicote, M. T. *Coord. Chem. Rev.* **1999**, 195, 1143–1161.

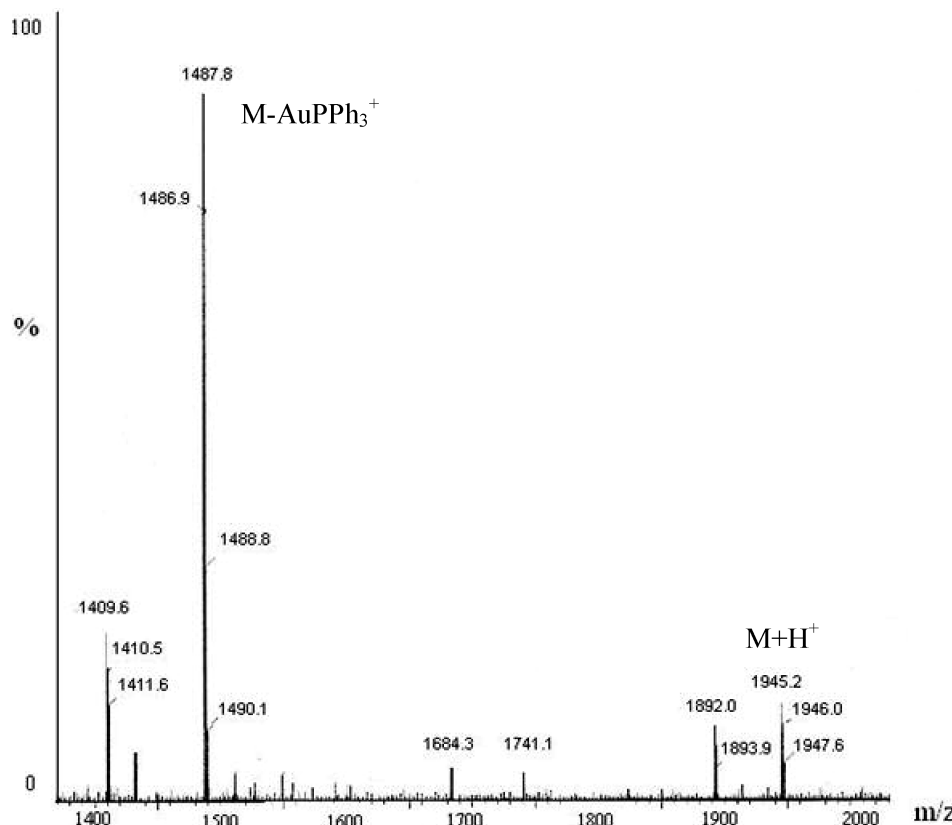
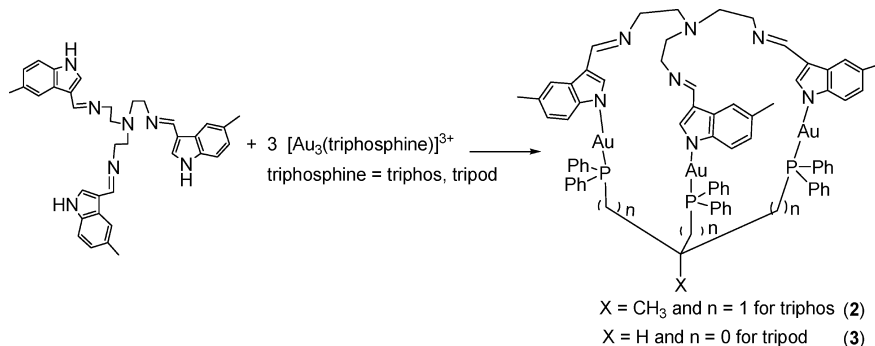


**Figure 1.** ESI-MS mass spectrum of compound **1**.

**Scheme 3**



derivative. The IR spectrum displays a lower stretching vibration energy of the indole rings ( $\Delta\bar{\nu} = 15 \text{ cm}^{-1}$ ) on coordination. ESI-MS shows the peak of the monoprotonated species [ $M + H^+$ ] at 1945.2 and those of the corresponding loss of  $\text{AuPPh}_3^+$  fragments (Figure 1).

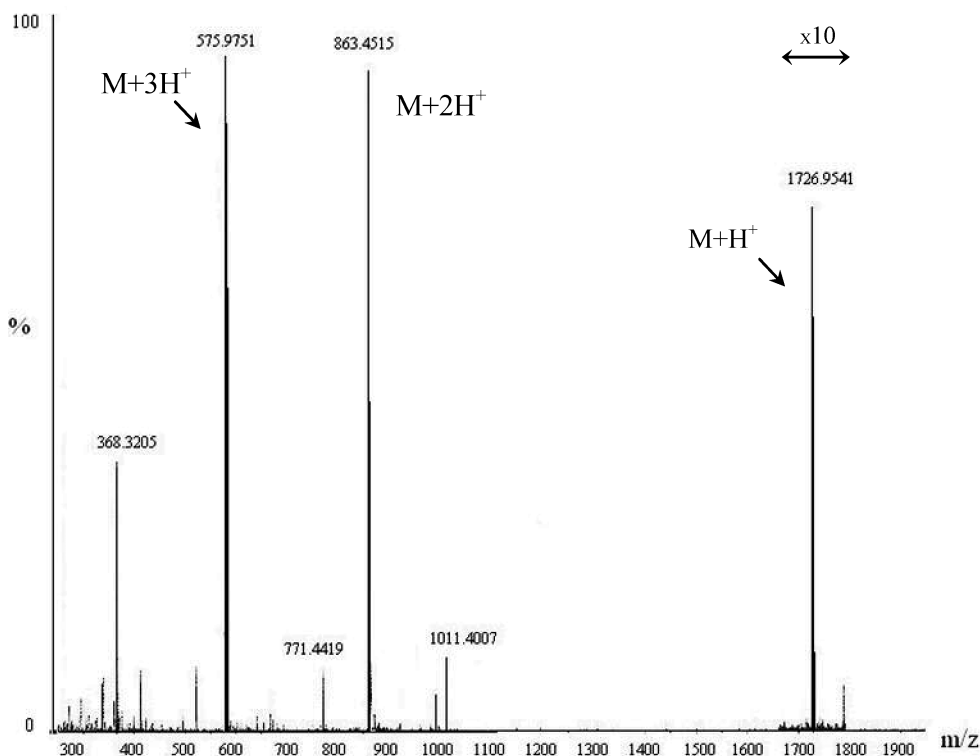
Because of the good reactivity of this new tripodal ligand with the gold triphenylphosphine fragment, we explored the possibility of constructing new polygold compounds, with a closed-shell cavity, built with flexible linkers, to generate pseudorigid metallocryptands that could be tested as the host in molecular recognition processes. With this goal, the reaction between  $L$  and two flexible gold(I) triphosphine derivatives was undertaken to obtain the two new metallocryptands **2** and **3** in excellent yields (Scheme 3).

Although **2** could be synthesized following methods A and B, only method B was successful for the formation of **3**, most probably because of the low solubility of the  $(\text{AuCl})_3(\text{tripod})$  derivative. As we have observed for compound **1**,  $^{31}\text{P}$  NMR

spectra display a single resonance at 17.2 and 37.3 ppm for compounds **2** and **3**, respectively, that are moved upfield upon coordination of the  $[\text{Au}_3(\text{triposphine})]^{3+}$  fragment. The upfield shift ( $\Delta\delta = 0.3 \text{ ppm}$ ) of the indole protons and the observed IR resonances, which are lower than in the case of free  $L$ , also confirm the coordination of the ligand.

ESI-MS shows the peaks corresponding to the mono-, di-, and triprotonated species (1782.6 [ $M + H^+$ ], 892.2 [ $M + 2H^+$ ], and 595.2 [ $M + 3H^+$ ]) for **2** and 1727.0 [ $M + H^+$ ]<sup>+</sup>, 863.8 [ $M + 2H^+$ ], and 576.0 [ $M + 3H^+$ ]) for **3** (Figure 2).

**DFT Geometry Optimization.** DFT calculations were employed in order to optimize the minimum energy geometry of the complexes, because attempts to grow suitable crystals for X-ray diffraction were unsuccessful. The phenyl groups of the phosphine ligands are modeled by methyls for compounds **2** and **3** (models **2m** and **3m**) and are retained in compound **1** (models **1a** and **1b**). Some relevant distances and angles are presented in Table 1.

**Figure 2.** ESI-MS mass spectrum of compound **3**.**Table 1.** Relevant Calculated Distances ( $\text{\AA}$ ) and Angles (deg) for Models of Complexes **1–3**

distance/angle	<b>1a</b>	<b>2m</b>	<b>3m</b>
Au...Au	16.325	3.672	4.137
N(imidazole)...N(imidazole)	13.905	4.842	5.535
Au–P	2.306	2.314	2.305
Au–N	2.033	2.041	2.024
P–P	19.101	4.270	3.156
P–Au–N	179	167	174

Compound **1** is computationally challenging because of its flexibility. An added difficulty is that its conformation is strongly influenced by the phenyl groups of the triphenylphosphines. Therefore, we have modeled **1** with the explicit inclusion of these groups. The DFT method used is too time demanding to afford an extensive conformational search. However, we have optimized two different conformations, an extended (with the  $\text{CH}_2\text{--CH}_2$  group of the InTREN ligand in the trans position) and a compact conformation (with the  $\text{CH}_2\text{--CH}_2$  group of the InTREN ligand in the cis position) that we have called **1a** and **1b**, respectively (Figure 3).

The flexibility and the large size of the molecule allowed us to locate structures converged only within the gradient threshold.<sup>65</sup> In vacuum, **1b** is 3 kcal/mol more stable than **1a**, but solvation effects reverse this situation dramatically, and **1a** is predicted to be 13 kcal/mol more stable than **1b**. This large difference allows us to be confident to say that **1a** will be the predominant conformer in solution.

The metallocryptands models **2m** and **3m** were also optimized by DFT (Figure 4).

Complexes **2m** and **3m** form a cavity where the distance between the gold atoms is 3.67 and 4.14  $\text{\AA}$ , respectively. These distances are longer than the ones found in aurophilic interactions, typically considered for Au...Au distances shorter than the sum of two van der Waals radii (3–3.5

$\text{\AA}$ ).<sup>66</sup> The relative geometry obtained may seem unexpected because the triphosphine ligand has larger interatomic distances among the P atoms in **2m** (4.27  $\text{\AA}$ ) than in **3m** (3.16  $\text{\AA}$ ). The reason for this is that the InTREN ligand is much more twisted with respect to the triphosphine in the former, as can be seen from Figure 4 and from the Au–P–P–Au dihedral angles, which are  $-56^\circ$  in **2** and  $-39^\circ$  in **3**. The twisting of these two subunits has also the consequence of a less linear N–Au–P bond in **2m** ( $167^\circ$ ) than in **3m** ( $174^\circ$ ). So, the cavity in **2m** is not larger, as one could expect from the size of the phosphine ligands. It is also worth pointing out that the lone pairs of the nitrogen atoms from the tertiary amines are located outside the cavity and this could influence the reactivity and the geometry of possible derivatives between the gold complexes and the metal cations (see below).

From the optimized geometry, one can also see that the substitution of phenyl with methyl groups does not affect the geometry of the complex because all phenyl groups would be pointing outward without any sterical clash. In fact, optimization with a smaller basis set and including the phenyls did not show relevant geometrical changes (data not shown).

**Photophysical Characterization.** Absorption spectra of compounds **1**, **3**, and their organic precursor, L, were recorded in freshly prepared dichloromethane solutions (Figure 5), and their main features are summarized in Table 2. The absorption spectrum of compound **2** was not undertaken due to the lack of solubility of this compound.

The electronic absorption spectrum of the InTREN precur-

(65) Gaussian03 also uses an estimated displacement to consider full convergence. But, because of the large size of this molecule and the use of a nonexact Hessian, this convergence criterium was difficult to meet even when the energy did not lower for several steps.

(66) Schmidbaur, H. *Chem. Soc. Rev.* **1995**, 24, 391.

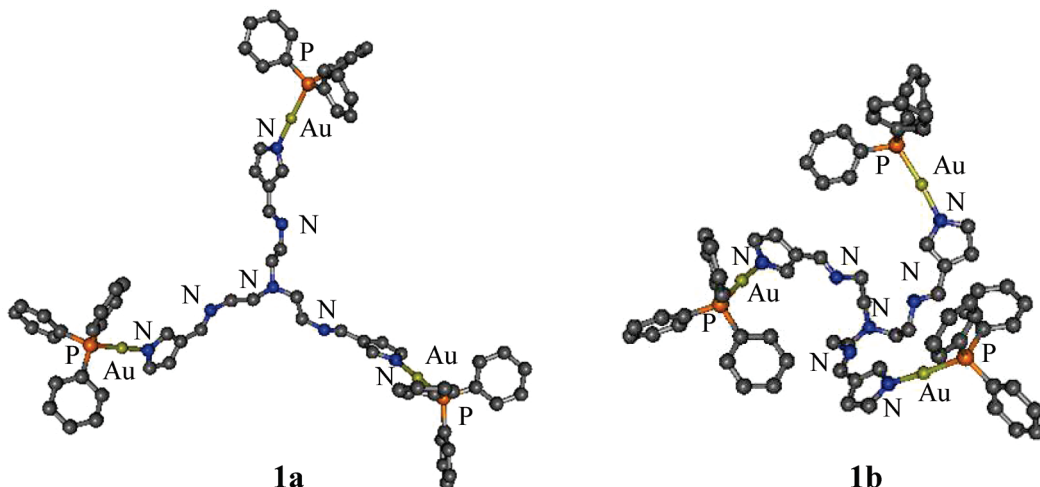


**Figure 3.** Minimized energy molecular structure of the model compound of **1** in its opened (**1a**) and closed (**1b**) possible conformations. Hydrogen atoms have been omitted for clarity.

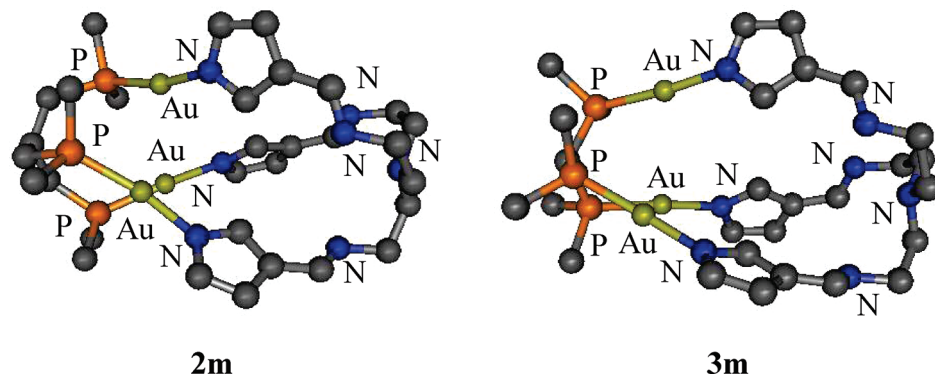


**Figure 4.** Minimized energy molecular structure of models **2m** and **3m**. Hydrogen atoms have been omitted for clarity.

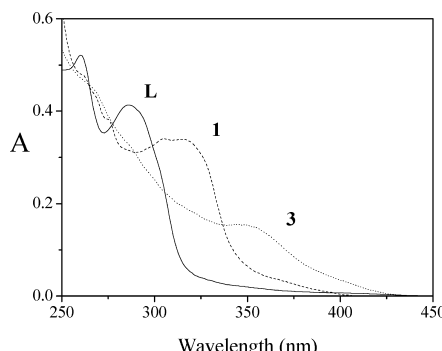


**Figure 5.** Absorption spectra in  $1 \times 10^{-5}$  M freshly prepared dichloromethane solution of compounds **1**, **3**, and free InTREN ligand (**L**).

sor shows the characteristic shape of the indole group attributed to the two close low-lying  $\pi\pi^*$  excited states  ${}^1\text{L}_\text{a}$  and  ${}^1\text{L}_\text{b}$  of this chromophore.<sup>50,67–69</sup> Absorption spectra of the gold derivatives **1** and **3** present their lowest energy band at longer wavelength with respect to the case of the organic ligand ( $\sim 310$  and  $350$  nm, respectively), and that band could be assigned as a ligand-to-metal charge transfer (LMCT) transition based on TD-DFT calculations (see below).

The emission of compounds **1** and **3** in dichloromethane solution is very weak (data not shown).

Excitation of the powders at  $360$  nm gives no luminescence for **L** and emission bands at  $564$ ,  $562$ , and  $597$  nm for the gold complexes **1–3** (Figure 6). The red shift displayed

**Table 2.** Electronic Absorption and Emission Data in  $1 \times 10^{-5}$  M Freshly Prepared Dichloromethane Solution, and Emission Maxima for the Powders at Room Temperature

compound	$\lambda_{\text{max}}/\text{nm}$ ( $10^{-3}\epsilon/\text{M}^{-1}\cdot\text{cm}^{-1}$ )	emission ( $\lambda_{\text{exc}} = 360$ nm)	
		$\lambda_{\text{max}}/\text{nm}$ ( $\text{CH}_2\text{Cl}_2$ )	$\lambda_{\text{max}}/\text{nm}$ (solid)
<b>1</b>	260 (46.4), 265 (43.8), 275 (37.0), 305 (34.0), 316 (33.9)	440, 520	564
<b>2</b>			562
<b>3</b>	260 (47.3), 285 sh (33.2), 315 (19.6), 350 (15.4), 390 (5.1)	415, 515 sh	597
<b>L</b>	262 (56.6), 286 (46.1), 300 sh (35.1)		

by **3**, as discussed for other luminescent gold compounds,<sup>54,71–84</sup> could be related with the presence of Au–Au interactions. However, in all three cases, the calculated Au–Au distances in the DFT optimized geometries are greater than those typically considered for the establishment of aurophilic interactions (Table 1).<sup>70</sup>

**TD-DFT Calculations.** DFT calculations have been carried out in order to know the geometry of the frontier orbitals of the gold complexes. Model compounds **1m**, **2m**, and **3m** where phenyl groups were substituted by methyls have been used for these calculations. The occupied orbitals are mostly localized in the central tertiary amine, and the lowest unoccupied molecular orbitals (LUMOs) have a large

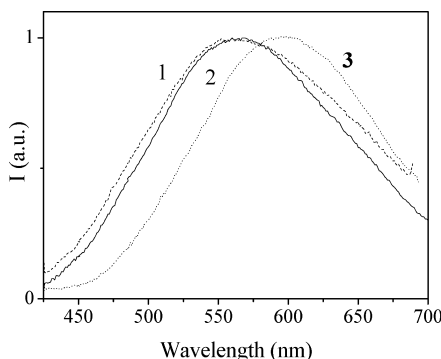


**Figure 6.** Normalized solid emission spectra of compounds **1–3** upon excitation of the samples at  $\lambda = 360$  nm.

contribution of the gold and the phosphine moieties and are Au–P antibonding. In the case of compound **1**, there is also a contribution of the indole group in these orbitals.

TD-DFT studies were performed in order to interpret the optical properties of these compounds. The most relevant calculated electronic transitions of the models are presented in Table 3 (compound **1m**), Table S1 in the Supporting Information (compound **2m**), and Table 4 (compound **3m**).

The low energy excitations obtained by this method are in the range 288–305 nm (**1m**), 333–395 nm (**2m**), and 335–386 nm (**3m**) including dichloromethane effects and are in good agreement with the recorded experimental data.

The experimental broad band at  $\sim 310$  nm of compound **1** is expected to have contributions from the two transitions with the higher oscillator strength value (calculated value: 306 nm; experimental value: 316 nm) and is assigned to a mixed transition from the highest occupied molecular orbital

- (67) Serrano-Andrés, L.; Roos, B. O. *J. Am. Chem. Soc.* **1996**, *118*, 185–195.
- (68) Borin, A. C.; Serrano-Andrés, L. *Chem. Phys.* **2000**, *262*, 253–265.
- (69) Sinha, S.; De, R.; Ganguly, T. *Spectrochim. Acta, Part A* **1998**, *54*, 145–157.
- (70) Schmidbaur, H. *Gold Bull. (London, U. K.)* **2000**, *33*, 3–10.
- (71) Bardaji, M.; de la Cruz, M. T.; Jones, P. G.; Laguna, A.; Martínez, J.; Villacampa, M. D. *Inorg. Chim. Acta* **2005**, *358*, 1365–1372.
- (72) Stott, T. L.; Wolf, M. O.; Patrick, B. O. *Inorg. Chem.* **2005**, *44*, 620–627.
- (73) Yam, V. W. W.; Cheung, K. L.; Yip, S. K.; Cheung, K. K. *J. Organomet. Chem.* **2003**, *681*, 196–209.
- (74) Ovejero, P.; Mayoral, M. J.; Cano, M.; Lagunas, M. C. *J. Organomet. Chem.* **2007**, *692*, 1690–1697.
- (75) Lee, Y. A.; Eisenberg, R. *J. Am. Chem. Soc.* **2003**, *125*, 7778–7779.
- (76) Mohamed, A. A.; López-de-Luzuriaga, J. M.; Fackler, J. P. *J. Cluster Sci.* **2003**, *14*, 61–70.
- (77) Zheng, S. L.; Nygren, C. L.; Messerschmidt, M.; Coppens, P. *Chem. Commun.* **2006**, 3711–3713.
- (78) van Zyl, W. E.; López-de-Luzuriaga, J. M.; Fackler, J. P. *J. Mol. Struct.* **2000**, *516*, 99–106.
- (79) van Zyl, W. E.; López-de-Luzuriaga, J. M.; Mohamed, A. A.; Staples, R. J.; Fackler, J. P. *Inorg. Chem.* **2002**, *41*, 4579–4589.
- (80) Pintado-Alba, A.; de la Riva, H.; Nieuwhuyzen, M.; Bautista, D.; Raithby, P. R.; Sparkes, H. A.; Teat, S. J.; López-de-Luzuriaga, J. M.; Lagunas, M. C. *Dalton Trans.* **2004**, 3459–3467.
- (81) Fernandez, E. J.; Gimeno, M. C.; Laguna, A.; López-de-Luzuriaga, J. M.; Monge, M.; Pyykkö, P.; Sundholm, D. *J. Am. Chem. Soc.* **2000**, *122*, 7287–7293.
- (82) Li, C. K.; Lu, X. X.; Wong, K. M. C.; Chan, C. L.; Zhu, N. Y.; Yam, V. W. W. *Inorg. Chem.* **2004**, *43*, 7421–7430.
- (83) Onaka, S.; Yaguchi, M.; Yamauchi, R.; Ozeki, T.; Ito, M.; Sunahara, T.; Sugura, Y.; Shiotsuka, M.; Horibe, M.; Okazaki, K.; Iida, A.; Chiba, H.; Inoue, K.; Imai, H.; Sako, K. *J. Organomet. Chem.* **2005**, *690*, 57–68.
- (84) Ferrer, M.; Gutierrez, A.; Rodriguez, L.; Rossell, O.; Lima, J. C.; Font-Bardía, M.; Solans, X. Submitted for publication.

**Table 3.** Calculated TD-DFT Low-Energy Singlet Excitation Energies, Wavelengths, and Oscillator Strengths (OS) and Experimental Data for Model **1m**

transition	<i>E</i> /nm	<i>E</i> /eV	$\lambda_{\text{max}}$ /nm	OS
H → L (58%), H → L+2 (24%)	306	4.06	316	0.182
H-1 → L+3 (33%), H → L+3 (17%)	298	4.17		0.003
H-1 → L (59%), H-1 → L+2 (15%)	289	4.29	305	0.319
H → L+3 (87%), H-2 → L+3 (13%)	283	4.38		0.001
H → L (58%), H-1 → L (27%), H-1 → L+2 (16%)	276	4.49	275	0.200
H-2 → L+2 (31%), H-1 → L (37%), H-2 → L (13%), H → L (12%)	273	4.53		0.056
H → L+2 (39%), H → L (38%), H-1 → L+2 (16%)	269	4.60	265	0.0852

**Table 4.** Calculated TD-DFT Low-Energy Singlet Excitation Energies, Wavelengths, and Oscillator Strengths (OS) for Model **3m**

transition	<i>E</i> /nm	<i>E</i> /eV	$\lambda_{\text{max}}$ /nm	OS
H → L (99%)	432	2.86		0.000
H-1 → L (33%), H-2 → L (66%)	386	3.21	390	0.001
H → L+1 (50%), H → L+2 (50%)	372	3.33		0.001
H-1 → L (20%), H → L+3 (34%), H-2 → L (13%), H-2 → L+2 (23%)	335	3.69	350	0.054
H-2 → L (32%)	327	3.79		0.033
H-2 → L+3 (61%), H-1 → L+3 (34%)	309	4.01	315	0.003

(HOMO) to the LUMO (58%) and LUMO+2 (24%). The second observed band (calculated value: 289 nm; experimental value: 305 nm) is a mixed transition from the HOMO–1 to the LUMO (59%) and L+2 (15%) orbitals. The involved orbitals in these transitions are represented in Figure 7.

The electronic density of the HOMO–1 orbital is mainly centered at the indole group while the central tertiary amine concentrates the electronic density of the HOMO orbital. The unoccupied orbitals are Au–P antibonding orbitals with a slight contribution of the indole groups. Assuming that DFT underestimates the Au contribution in the virtual orbitals,<sup>85</sup> the lower energy electronic transition could be mainly attributed to a LMCT N(p, tertiary amine) → Au mixed with an indole → Au transition.

The LMCT N(p, tertiary amine) → Au transition has also been calculated to be responsible for the lowest-energy transitions for compounds **2** and **3**. These complexes present a closed-conformation structure by the substitution of the triphenylphosphine ligands of **1** by a triphosphine. Although the absorption spectrum of **2** has not been recorded, the predicted electronic transition and the involved orbitals have also been calculated (see the Supporting Information). The calculated transitions with higher oscillator strength are also in good agreement with the experimental results for compound **3m**. Thus, the experimental band at  $\sim 350$  nm is calculated at 335 nm. The absorption is assigned to a mixed transition from the HOMO–2, HOMO–1, and HOMO orbitals to the LUMO, LUMO+2, and LUMO+3. The three-dimensional representation of these orbitals is presented in Figure 8.

The large Stokes shift between absorption and emission suggests triplet contribution to the emission.

(85) Costa, P. J.; Calhorda, M. J. *Inorg. Chim. Acta* **2006**, *359*, 3617–3624.

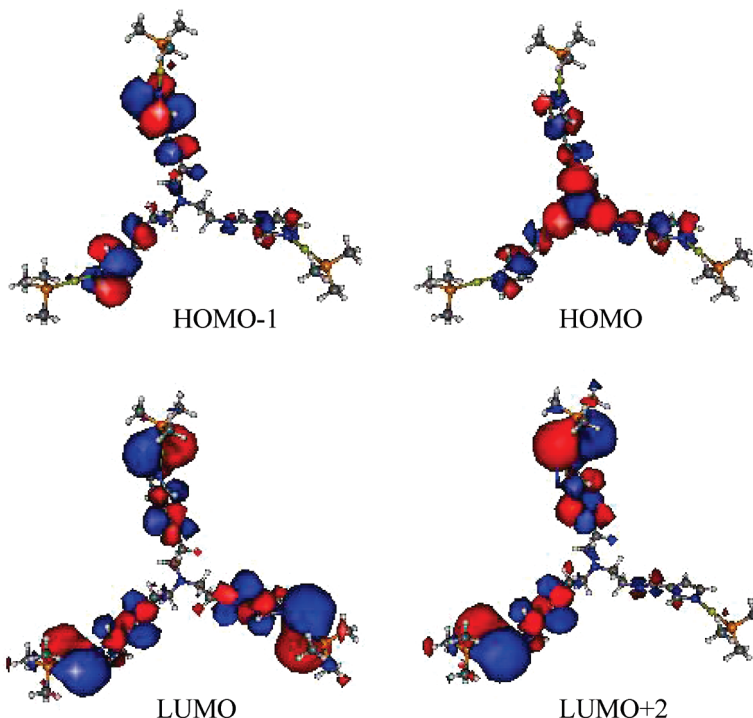


**Figure 7.** Isodensity representation of the orbitals of the model **1m** of complex **1** involved in the lowest energy transitions.

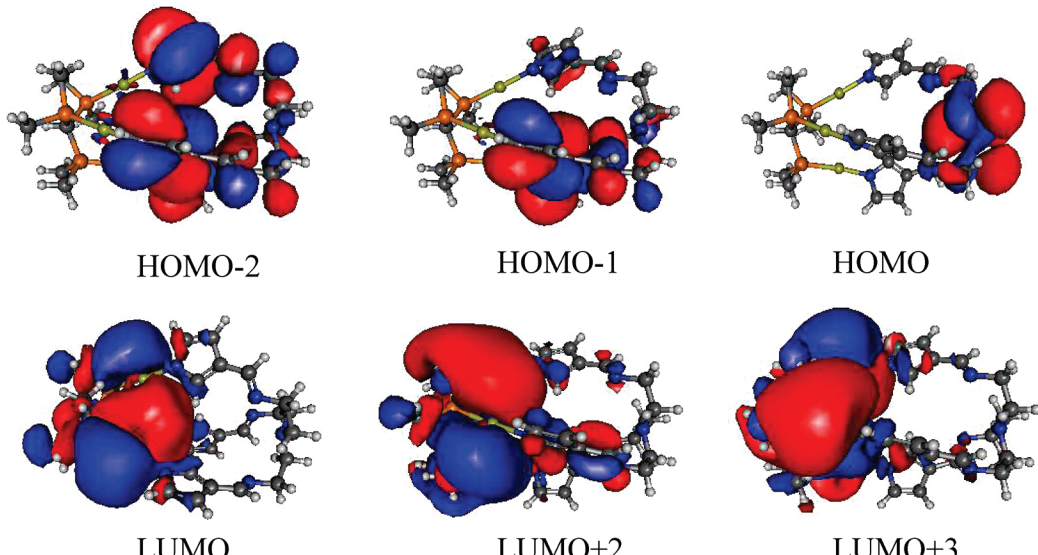


**Figure 8.** Isodensity representation of the orbitals of the model **3m** of complex **3** involved in the lowest energy transitions.

**Molecular Recognition Studies of Metal Cations in Solution.** Molecular recognition of metal cations constitutes a potential application for these compounds.<sup>86–88</sup> With this goal in mind, titrations of **1** and **3** with Zn<sup>2+</sup>, Ni<sup>2+</sup>, and Cu<sup>2+</sup> salts were undertaken in dichloromethane solution, and changes in their electronic spectra were recorded.

The addition of different amounts of the corresponding triflate or tetrafluoroborate salts to a  $1 \times 10^{-5}$  M solution

of the dendritic compound **1** conduced to a decrease of the lowest energy absorption band at  $\sim 310$  nm and the formation of a new band at longer wavelengths ( $\sim 350$  nm, see Figure 9).

The representation of the variation maxima as a function of the number of Zn<sup>2+</sup> equivalents added to the solution leads us to conclude the formation of a 1:1 complex between the gold derivative and the metal atom (Figure 9, inset). The affinity of these metals to coordinate with amines suggests that the metal atom could coordinate to the secondary amines of the InTREN ligand. This fact is supported by the results obtained with the free InTREN ligand. The Zn<sup>2+</sup> derivative of this precursor was isolated and characterized, and the recorded IR spectrum clearly indicates the coordination by

(86) Liang, Z.; Liu, Z. L.; Gao, Y. H. *Tetrahedron Lett.* **2007**, *48*, 3587–3590.

(87) Ipe, B. I.; Yoosaf, K.; Thomas, K. G. *J. Am. Chem. Soc.* **2006**, *128*, 1907–1913.

(88) Tamayo, A.; Pedras, B.; Lodeiro, C.; Escriche, L.; Casabo, J.; Capelo, J. L.; Covelo, B.; Kivekas, R.; Sillanpaa, R. *Inorg. Chem.* **2007**, *46*, 7818–7826.

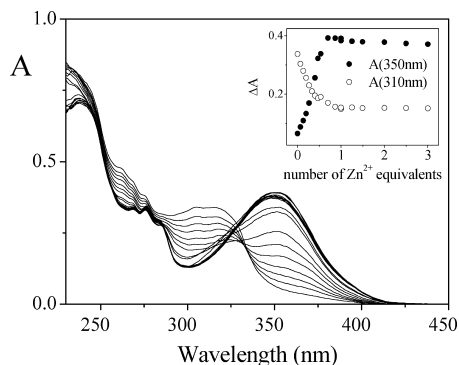


**Figure 9.** Absorption spectra of compound **1** in the presence of 1–3 equiv of  $Zn^{2+}$  in dichloromethane solution ( $[1] = 1 \times 10^{-5}$  M,  $[Zn^{2+}] = 1 \times 10^{-4}$  M).

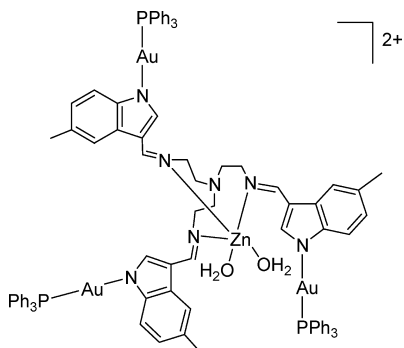


**Figure 10.** ChemDraw representation of the new supramolecular compound obtained by the titration of the dendrimer **1** with  $Zn(OTf)_2$ .

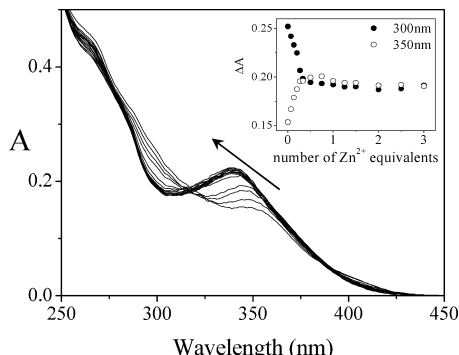


**Figure 11.** Absorption spectra of compound **3** in the presence of 1–3 equiv of  $Zn^{2+}$  in dichloromethane solution ( $[3] = 1 \times 10^{-5}$  M;  $[Zn^{2+}] = 1 \times 10^{-4}$  M).

the secondary amines.<sup>50</sup> Moreover, X-ray crystal structures of other similar tripodal compounds show the coordination with metal atoms by the secondary amines.<sup>89</sup> These reported results strongly suggest that the same coordination occurs with the gold derivative **1** (Figure 10). On the other hand, the coordination with the  $Zn^{2+}$  increases the electron deficient character of the environment in the direction of the charge transfer, which is in agreement with the observed red shift of the band for the LMCT transition.

Similar experiments carried out with a  $1 \times 10^{-5}$  M dichloromethane solution of the metallocryptand **3** show the opposite effect (Figure 11). In this case, the addition of different quantities of the metal solution leads to the

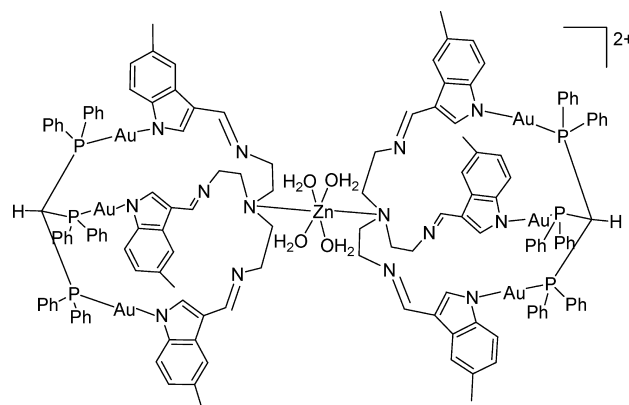


**Figure 12.** ChemDraw representation of the new supramolecular compound with sandwich structure obtained by the titration of the metallocryptand **3** with  $Zn(OTf)_2$ .

formation of a new blue-shifted band while a valley appears at 300 nm. The recorded changes in absorption as a function of metal ion concentration reach a plateau at 0.5 equiv of metal ion that indicates the formation of a 1:2 complex (Figure 11, inset).

These results are clearly different from those obtained for the dendrimeric derivative. The recorded blue-shifted band suggests that in this case the charge transfer process is less favored; that is, it suggests complexation involving the tertiary amine. On the other hand, the formation of a complex with 1:2 stoichiometry,  $Zn^{2+}/\mathbf{3}$ , also points to the formation of a compound with a different structure. The HOMO electronic density of the metallocryptand is mainly located in the tertiary amine with the lone pairs of the InTREN ligand pointing outside the cavity and a single coordinative bond that will not stabilize the formation of the new complex with the  $Zn^{2+}$ . This is probably one of the reasons why complexation with  $Zn^{2+}$  leads to the formation of a complex with 2:1 stoichiometry. A possible structure is exemplified in Figure 12.

High resolution ESI-MS and MALDI-TOF-MS have been very useful to verify the formation of these new heterometallic complexes. The recorded mass spectrum for a 1:1  $\mathbf{3}/Zn^{2+}$  dichloromethane solution confirms the formation of the  $\mathbf{3}\cdot Zn^{2+}\cdot \mathbf{3}$  species with sandwich structure with peaks at  $m/z = 1194.9$ , 1178.6, and 887.3 that correspond to the  $[\mathbf{3}\cdot Zn(H_2O)_4\cdot \mathbf{3} + H^+]^{3+}$ , the  $[\mathbf{3}\cdot Zn(H_2O)\cdot \mathbf{3} + H^+]^{3+}$ , and the  $[\mathbf{3}\cdot Zn(H_2O)_2\cdot \mathbf{3} + 2H^+]^{4+}$  fragments.

The mass spectrum recorded for a 1:1  $\mathbf{1}\cdot Zn^{2+}$  dichloromethane solution shows peaks at  $m/z = 1022.2$  and 1013.9 indicative of the presence of the  $[\mathbf{1}\cdot Zn(H_2O)_2]^{2+}$  and the  $[\mathbf{1}\cdot Zn(H_2O)]^{2+}$  species. These results are in agreement with spectroscopic data, since absorption variations recorded at the maxima reach a plateau with 1 equiv of  $Zn^{2+}$  in the case of compound **1** and with 0.5 equiv in the case of **3**.

Similar results were obtained in the titrations of **1** and **3** with  $Ni^{2+}$  and  $Cu^{2+}$  salts.

## Conclusions

Self-assembly reactions between the tris-indole InTREN ligand (**L**) and the gold(I) phosphine fragments lead to the construction of new gold(I) complexes by two different

(89) Nakamura, H.; Fujii, M.; Sunatsuki, Y.; Kojima, M.; Matsumoto, N. *Eur. J. Inorg. Chem.* **2008**, 1258–1267.

methods. A metallocendrimer-like complex (**1**) has been synthesized when the  $\text{AuPPh}_3^+$  fragment is used, and two neutral gold(I) metallocryptands with empty cavities (**2** and **3**) have been constructed when the chosen gold fragments are  $[\text{Au}_3(\text{triphenylphosphine})]^{3+}$  derivatives with different lengths.

Density functional theory (B3LYP) has been used to optimize the minimum energy geometry of the complexes. TD-DFT has been a very useful tool to attribute the absorption bands to LMCT  $\text{N}(\text{p}, \text{tertiary amine}) \rightarrow \text{Au}$  transitions. Emission in the solid state seems to originate from the  ${}^3\text{LMCT}$  state.

Spectroscopic titrations with metals of **1** and **3** dichloromethane solutions conduce to the formation of new heterometallic compounds with different structures in both cases. While the dendrimeric species mainly gives the 1:1 complex with coordination of the secondary amines, compound **3** leads to the formation of a new  $\mathbf{3}\cdot\mathbf{M}^{2+}\cdot\mathbf{3}$  heterometallic sandwich type structure with 2:1 stoichiometry. The evidence is supported by spectroscopy, mass spectrometry, and DFT calculations.

**Acknowledgment.** We are indebted to FEDER/Fundaçāo para a Ciēncia e Tecnologia (Portugal) PTDC/QUI/66250/

2006 for financial support and to the Ministerio de Educaciōn y Ciencia (Spain) for the Project CTQ2006-02362/BQU, Acciōn Integrada Hispano-Portuguesa HP2006-0101, and CRUP (Portugal) Acção Integrada Luso-Espanhola E-68/07. L.R. acknowledges the postdoctoral grant given by the Fundaçāo para a Ciēncia e Tecnologia (Portugal, SFRH/BPD/26882/2006). R.C. thanks the Spanish Ramón y Cajal program for financial support. This research has been partly performed using the CESCA resources. The authors also would like to thank Dr. Montserrat Ferrer and Dr. Oriol Rossell from the Inorganic Departament of the Universitat de Barcelona for fruitful discussions.

**Supporting Information Available:** ESI-MS mass spectrum of compound **2** (Figure S1), table with calculated TD-DFT low-energy singlet excitation energies, wavelengths, and oscillator strengths for model **2m** (Table S1), and isodensity representation of the orbitals of model **2m** involved in the lowest energy transitions of compound **2** (Figure S2). This material is available free of charge via the Internet at <http://pubs.acs.org>.

IC800266M